Growth and spectral characterization of Er^{3+}-doped $(Sr_{0.7}Ca_{0.3})_3Y(BO_3)_3$ crystal

LEI WU[a,b], ZHOUBIN LIN[a], LIZHEN ZHANG[a], YISHENG HUANG[a], GUOFU WANG[a,*]
[a]*Key Laboratory of Optoelectronics Material Chemistry and Physics, Fujian Institute of Research on the Structure of Matter, Chinese Academy of Sciences, Fuzhou, Fujian 350002, China*
[b]*Graduate School of Chinese Academy of Science, Beijing 100037, China*

Er^{3+}:$(Sr_{0.7}Ca_{0.3})_3Y(BO_3)_3$ crystal with dimensions of ϕ 21×34 mm^3 has been grown by the Czochralski method. The polarized spectral properties were investigated. Based on the Judd-Ofelt theory, the oscillator strength parameters, transition probability, fluorescence branching ratio and radiative lifetime were estimated. The stimulated emission cross-sections of Er^{3+}:$(Sr_{0.7}Ca_{0.3})_3Y(BO_3)_3$ crystal were calculated to be $21.0\times10^{-21}cm^2$ at 1541nm for the π-polarization and $2.25\times10^{-20}cm^2$ at 1536nm for the σ-polarization. The quantum efficiency η_c, Er^{3+}:$(Sr_{0.7}Ca_{0.3})_3Y(BO_3)_3$ crystal is 40.3%. In comparison with Er^{3+}:$Sr_3Y(BO_3)_3$ crystal, the spectral properties of Er^{3+}:$(Sr_{0.7}Ca_{0.3})_3Y(BO_3)_3$ crystal are better than that of $Sr_3Y(BO_3)_3$ crystal. The investigated results showed that after the Ca^{2+} ion partly substitute for Sr^{2+} ion in $Sr_3Y(BO_3)_3$ crystal to form the $(Sr_{0.7}Ca_{0.3})_3Y(BO_3)_3$ solid solution, it can greatly improve the quantum efficiency η of Er^{3+}:$(Sr_{0.7}Ca_{0.3})_3Y(BO_3)_3$ crystal. Therefore, Er^{3+}:$(Sr_{0.7}Ca_{0.3})_3Y(BO_3)_3$ crystal may be become a 1.55 μm laser crystal materials.

(Received April 29, 2012; accepted July 19, 2012)

Keywords: Laser crystal, Crystal growth, Spectral properties, Er^{3+}:$(Sr_{0.7}Ca_{0.3})_3Y(BO_3)_3$ crystal

1. Introduction

Since the 1.55 μm laser of Er^{3+} ions through $^4I_{13/2} \rightarrow {}^4I_{15/2}$ transition has wide applications in optical communication technology, medical and eye-safe laser, the Er^{3+}-doped laser materials have attracted much attention. Up to now, the spectral properties of Er^{3+} ions in many materials have been widely investigated, such as YVO_4 [1], $Y_3Al_5O_{12}$ [2], $YAlO_3$ [3], $KGd(WO_4)_2$ [4], $KY(WO_4)_2$ [5] and $NaY(MoO_4)_2$ [6].

The $M_3Re(BO_3)_3$ (M = Ba, Sr, Ca; Re=La-Lu, Y, Sc) compound belongs to the hexagonal system with space group $R3$. The $M_3Re(BO_3)_3$ (M = Ba, Sr, Ca; Re=La-Lu, Y, Sc) crystals are regarded as potential laser host material owing to their good chemical, physical and spectral properties. [7-13]. The $Sr_3Y(BO_3)_3$ crystal is a member of $M_3Re(BO_4)_3$ (M = Ba, Sr, Ca; Re=La-Lu, Y, Sc) family. Recently, it was found that when the Ca^{2+} ions partly were substituted for the Sr^{2+} ions in $(Sr_{0.7}Ca_{0.3})_3Y(BO_3)_3$ crystal to form the solid solutions $(Sr_{0.7}Ca_{0.3})_3Y(BO_3)_3$, the Yb^{3+}-doped $Sr_3Y(BO_3)_3$ solid solution showed good spectral properties [14]. Recently, our laboratory has investigated the Er^{3+}-doped $Sr_3Y(BO_3)_3$ crystal, the investigated results showed that Er^{3+}:$Sr_3Y(BO_3)_3$ crystal may be regarded as a potential laser host materials for 1.55 μm laser [15]. In order to improve further the spectral properties of Er^{3+}:$Sr_3Y(BO_3)_3$ crystal, we hope that when the Ca^{2+} ion partly substitute for Sr^{2+} ion to form the $(Sr_{0.7}Ca_{0.3})_3Y(BO_3)_3$ solid solution, it can improve the spectral properties. To explore new more efficient Er^{3+} laser crystal, this paper reports the growth and spectral properties of Er^{3+}-doped $(Sr_{0.7}Ca_{0.3})_3Y(BO_3)_3$ crystal.

2. Experiment

Since the $Sr_3Y(BO_3)_3$ crystal melts congruently at 1400°C [10], Er^{3+}-doped $(Sr_{0.7}Ca_{0.3})_3Y(BO_3)_3$ crystal can be grown by Czochralski method. The chemicals used were Sr_2CO_3, $CaCO_3$, Y_2O_3, H_3BO_3 and Er_2O_3 with purity of 99.99%. The raw materials were synthesized by the solid-state reaction method. The raw materials were weighed accurately according to the stoichiometric ratio of $(Sr_{0.7}Ca_{0.3})_3Y_{0.97}Er_{0.03}(BO_3)_3$. A 3wt% excess amount of H_3BO_3 was added to compensate the loss of B_2O_3 volatilization in the process of the solid-state and growth. The weighed raw materials were ground and extruded to form pieces. Then pieces were placed in a platinum crucible and held to 900℃ for 24 h. The process was repeated once again to assure adequate solid-state reaction. The synthesized raw materials were placed in an iridium crucible with dimension of ϕ 45×40 mm^3. The crystal was grown by Czochralski method in a 2.5 kHz frequency induction furnace in N_2 atmosphere. The full charged crucible was placed into the furnace and slowly heated up to 1500°C. The melt was held at 1500°C for 2 h to evacuate the bubbles out of the melt. After repeating

seeding and adjusting the growth temperature to about 1400°C, the crystal was grown using a pulling rates of 1mm/h and a rotating rate of 15 rpm. When growth process ended, the grown crystal was drawn from the melt and slowly cooled to room temperature at a cooling rate of 15°C/h.

A sample cut from the as-grown crystal (Fig. 1(b)) along c-axis was used to measure the absorption and emission spectra of Er^{3+}:$(Sr_{0.7}Ca_{0.3})_3Y(BO_3)_3$ crystal. The polarized absorption spectra were measured using a Perkin-Elmer UV-vis-NIR spectrometer (Lambda-900) in range of 300-1700nm at room temperature. The polarized fluorescence spectra and fluorescence lifetime were measured using an Edinburgh Instruments FLS920 spectrophotometer with a continuous Xe-flash lamp as a light. In the experiment the π- and σ-polarizations are defined in terms of the E-vector being parallel or perpendicular to the c-axis, respectively.

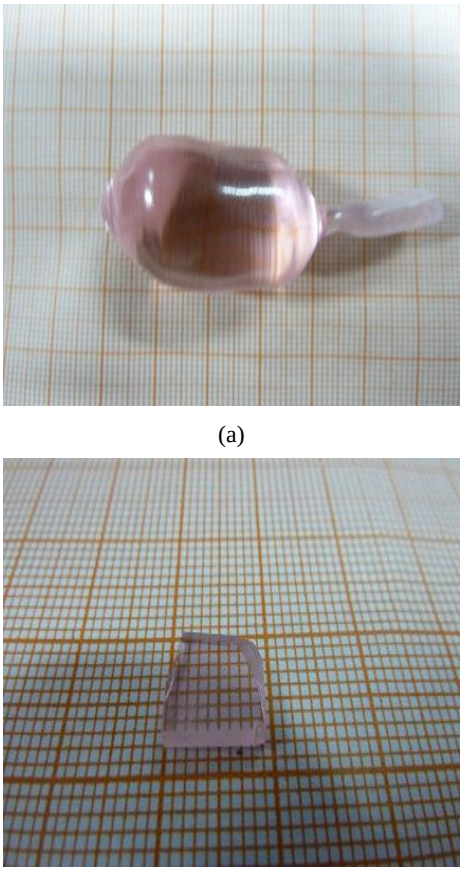

(a)

(b)

Fig. 1. (a) As-grown Er^{3+}:$(Sr_{0.7}Ca_{0.3})_3Y(BO_3)_3$ crystal; (b) Polished sample of Er^{3+}:$(Sr_{0.7}Ca_{0.3})_3Y(BO_3)_3$ crystal.

3. Results and discussion

3.1 Crystal growth

Er^{3+}:$(Sr_{0.7}Ca_{0.3})_3Y(BO_3)_3$ crystal with dimensions of ϕ 21×34 mm^3 was obtained, as shown in Fig.1 (a). The concentration of Er^{3+} in the Er^{3+}:$(Sr_{0.7}Ca_{0.3})_3Y(BO_3)_3$ crystal was measured to be 2.80 at.% (i. e. 1.49×10^{-20} ions/cm^3) by inductively coupled plasma atomic emission spectroscopy (ICP-AES). The segregation coefficient of Er^{3+} in Er^{3+}:$(Sr_{0.7}Ca_{0.3})_3Y(BO_3)_3$ crystal was calculated to be 0.93 by the following formula:

$$k_{eff} = \frac{k_e}{k_0} \tag{1}$$

where k_e and k_0 are the concentrations of Er^{3+} ions in the solid and liquid phase, respectively.

3.2 Absorption spectra and Judd-Ofelt analysis

Fig. 2 shows the polarized absorption spectra of the 2.80 at. % Er^{3+}-doped $(Sr_{0.7}Ca_{0.3})_3Y(BO_3)_3$ crystal. The observed 9 absorption lines around 376, 407, 450, 488, 524, 655, 801, 974, and 1516 nm are assigned to transitions from the $^4I_{15/2}$ ground to the $^4G_{9/2}$+$^4G_{11/2}$, $^2H_{9/2}$, $^4F_{3/2}$, $^4F_{5/2}$, $^2H_{11/2}$, $^4F_{9/2}$, $^4I_{9/2}$, $^4I_{11/2}$, and $^4I_{13/2}$ excited state in proper order.

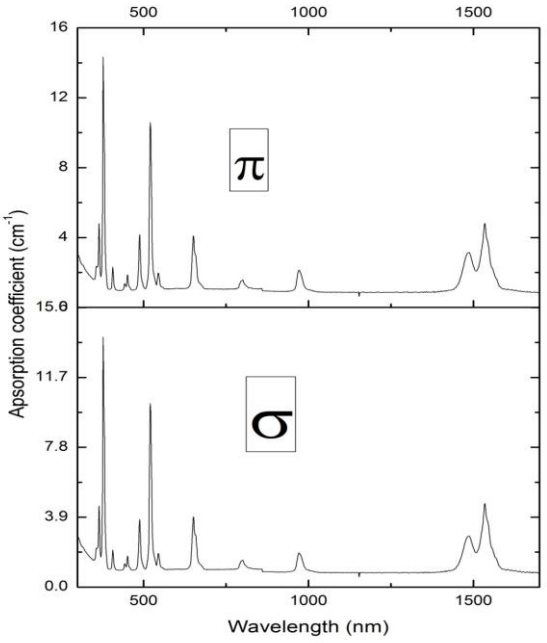

Fig. 2. Polarized absorption spectra of Er^{3+}:$(Sr_{0.7}Ca_{0.3})_3Y(BO_3)_3$ crystal at room temperature.

The absorption cross-section σ_{ab} was determined using $\sigma_{ab}= \alpha/N_c$ formula, where α is absorption coefficient, N_c is the concentration of Er^{3+} ions in Er^{3+}:$(Sr_{0.7}Ca_{0.3})_3Y(BO_3)_3$ crystal. The absorption cross-section σ_{ab} at 524, 970 nm are 6.02×10^{-20} cm^2 and 1.30×10^{-20} cm^2 for σ-polarization, and σ_{ab} at 524, 970 nm are 6.04×10^{-20} cm^2 and 1.44×10^{-20} for π-polarization, respectively.

Based on Judd-Ofelt theory [15, 17], the data of absorption spectra can be used to predict the oscillator strength parameter Ω_t, radiative lifetime τ_{rad}, branching rations β and transition probability A. The calculating procedures follow those described elsewhere [18-20]. The calculated results are listed in Table 1, 2 and 3, including first measured the line oscillator strength f_{mea} of the transitions between the ground $^4I_{15/2}$ (J=15/2) manifold and the excited J'-manifold.

Table 1. Oscillator strength parameters and emission cross-sections of Er^{3+} in Er^{3+}:$(Sr_{0.7}Ca_{0.3})_3Y(BO_3)_3$ and other Er^{3+}-doped crystals.

crystal		Ω_2 (10^{-20} cm^2)	Ω_4 (10^{-20} cm^2)	Ω_6 (10^{-20} cm^2)	σ_{em} (10^{-21} cm^2)	η_c (%)	Ref.
$Sr_3Y(BO_3)_3$	π	1.71	1.39	0.74	4.75	7.9	[15]
	σ	1.77	1.44	0.65	6.30		
YAG		0.45	0.98	0.62	4.5		[24]
$La_2(WO_4)_3$		7.20	1.05	0.31	4.14		[25]
$Ca_3La_2(BO_3)_4$		7.18	3.27	2.79	9.06		[26]
$(Ca_{0.3}Sr_{0.7})_3Y(BO_3)_3$	π	14.7	4.95	5.17	21.0	40.3	This work
	σ	14.9	4.59	5.64	22.5		

Table 2. Experimental and calculated line oscillator strengths of Er^{3+} in Er^{3+}:$(Sr_{0.7}Ca_{0.3})_3Y(BO_3)_3$ crystal (in units of 10^{-6}).

Transitions	π- Polarization			σ-Polarization		
	Λ (nm)	f_{exp}	f_{cal}	λ (nm)	f_{exp}	f_{cal}
$^4I_{13/2}$	1516	6.29	5.84	1518	6.84	6.27
$^4I_{11/2}$	974	1.83	2.70	975	1.96	2.90
$^4I_{9/2}$	801	1.04	1.21	801	1.00	1.14
$^4F_{9/2}$	655	7.83	8.22	655	7.82	8.26
$^2H_{11/2}$	524	2.48	2.65	524	2.47	2.66
$^4F_{5/2}$	488	7.45	8.68	488	7.60	9.19
$^4F_{3/2}$	450	2.94	4.30	450	2.82	4.69
$^2H_{9/2}$	407	3.00	3.30	407	2.94	3.56
$^4G_{9/2}$, $^4G_{11/2}$	376	5.45	5.26	376	5.48	5.28
rms(Δf)		1.34×10^{-6}			1.61×10^{-6}	
rms error		6.62%			7.92%	

Table 3. Calculated transition probabilities, radiative lifetime and branching ratios of Er^{3+} in Er^{3+}:$(Sr_{0.7}Ca_{0.3})_3Y(BO_3)_3$ crystal.

Transition J→J′	λ(nm)	A_{ed}(s^{-1})	A_{md}(s^{-1})	A_{total}(s^{-1})	β	τ_{rad}(ms)
$^4I_{13/2}\rightarrow{}^4I_{15/2}$	1543	577.029	48.458	625.489	1	1.599
$^4I_{11/2}\rightarrow{}^4I_{13/2}$	2746	99.364	10.821	874.251	12.603	1.144
$\rightarrow{}^4I_{15/2}$	988	764.065			87.396	
$^4I_{9/2}\rightarrow{}^4I_{13/2}$	1703	275.976		816.018	33.820	1.225
$\rightarrow{}^4I_{15/2}$	809	534.549			65.507	
$^4F_{9/2}\rightarrow{}^4I_{9/2}$	3466	16.771	3.348	6649.885	0.302	0.1503
$\rightarrow{}^4I_{11/2}$	1956	371.714	7.601		5.704	
$\rightarrow{}^4I_{13/2}$	1142	281.264			4.229	
$\rightarrow{}^4I_{15/2}$	656	5969.187			89.763	
$^4S_{3/2}\rightarrow{}^4I_{9/2}$	1665	323.637		9675.470	3.345	0.1033
$\rightarrow{}^4I_{11/2}$	1215	202.543			2.093	
$\rightarrow{}^4I_{13/2}$	842	2272.226			28.135	
$\rightarrow{}^4I_{15/2}$	545	6422.591			66.384	

3.3 Fluorescence spectra and stimulated emission cross-section

Fig. 3 displays the polarized fluorescence spectra of Er^{3+}:$(Sr_{0.7}Ca_{0.3})_3Y(BO_3)_3$ at room temperature, which was excited by the 521nm radiation. The broad emission band extends from 1450 to 1645 nm corresponding to the $^4I_{13/2}$ → $^4I_{15/2}$ transitions of Er^{3+} ion. The stimulated emission cross-sections σ_{em} (λ) can be estimated from the fluorescence spectra using the following Füchtbauer-Ladenburg (FL) formula [21]:

$$\sigma_{em}(\lambda)=\frac{3\lambda^5\beta I(\lambda)}{8\pi cn^2\tau_r\int\lambda[I_X(\lambda)+I_Y(\lambda)+I_Z(\lambda)]d\lambda}, \quad (15)$$

where I(λ) is the fluorescence intensity at wavelength λ, τ_r is the radiative lifetime, and β is the branching ratio, which equates to 1 for the $^4I_{13/2}\rightarrow{}^4I_{15/2}$ transition of Er^{3+}. Using the parameters obtained above, the stimulated emission cross-sections of Er^{3+}:$(Sr_{0.7}Ca_{0.3})_3Y(BO_3)_3$ crystal can be estimated. The stimulated emission cross-sections of the $^4I_{13/2}\rightarrow{}^4I_{15/2}$ transition at various wavelengths are shown in Fig. 4. The stimulated emission cross-sections σ_{em} (λ) of Er^{3+}:$(Sr_{0.7}Ca_{0.3})_3Y(BO_3)_3$ crystal were calculated to be $21.0\times10^{-21}cm^2$ at 1541 nm for the π-polarization and $2.25\times10^{-20}cm^2$ at 1536 nm for the σ-polarization, respectively.

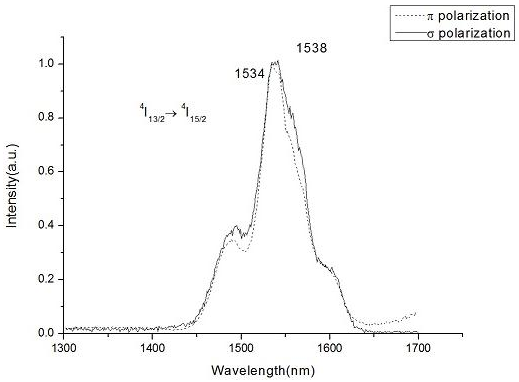

Fig. 3. Polarized fluorescence spectra of Er^{3+}:$(Sr_{0.7}Ca_{0.3})_3Y(BO_3)_3$ crystal excited by 521 nm radiation at room temperature.

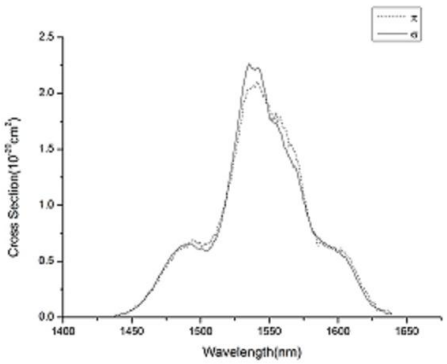

Fig. 4. Polarized emission cross-section for the $^4I_{13/2}\rightarrow{}^4I_{15/2}$ transition of Er^{3+}:$(Sr_{0.7}Ca_{0.3})_3Y(BO_3)_3$ crystal at room temperature.

Since the Er^{3+} laser via the $^4I_{13/2}\rightarrow{}^4I_{15/2}$ transition operates in a three-level scheme, the emission spectra are not sufficient to predict which of the polarizations exhibit higher gain. This can be determined by calculating the gain cross-section according to [22]:

$$\sigma_{gain}(\lambda)=\beta\sigma_{em}(\lambda)-(1-\beta)\sigma_{abs}(\lambda), \qquad (16)$$

where β is the ratio of the inverted ions to the total Er^{3+}-ion density. The relations between the calculated polarized gain cross section and wavelength in two polarizations with different β values (β = 0.1, 0.3, 0.5, 0.7, 0.9) is shown in Fig. 5. Laser gain is expected to occur only when $\sigma_{gain}(\lambda) > 0$ [23]. In Er^{3+}:$(Sr_{0.7}Ca_{0.3})_3Y(BO_3)_3$ crystal, a laser gain in the eye-safe range window is possible for $\beta \geq 0.5$. Generally speaking, the gain cross section is larger on the long wavelength edge, where reabsorption losses are small. Fig. 5 shows that the gain cross-section $\sigma_{gain}(\lambda) > 0$ for β=0.5, so laser emission can be realized in a wild range of 1535 nm to 1625 nm, which is available for use of tunable and ultra short laser.

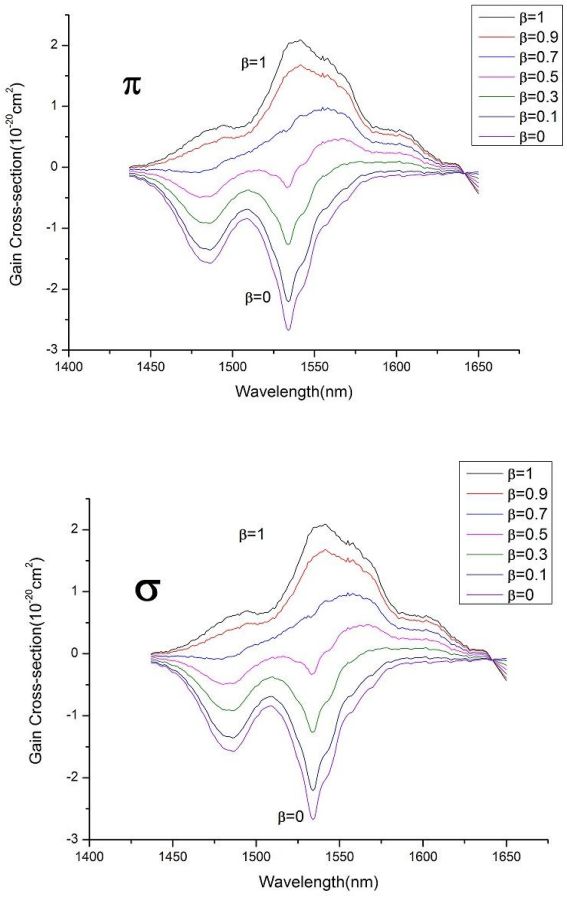

Fig. 5. Fain cross-section of Er^{3+}:$(Sr_{0.7}Ca_{0.3})_3Y(BO_3)_3$ crystal for both polarizations.

The fluorescence lifetime τ_f of $^4I_{13/2}\rightarrow{}^4I_{15/2}$ transition was measured to be 0.645 ms at room temperature (Fig. 6). Thus, the quantum efficiency η_c, which is defined as $\eta_c = \tau_f/\tau_r$, is 40.3%.

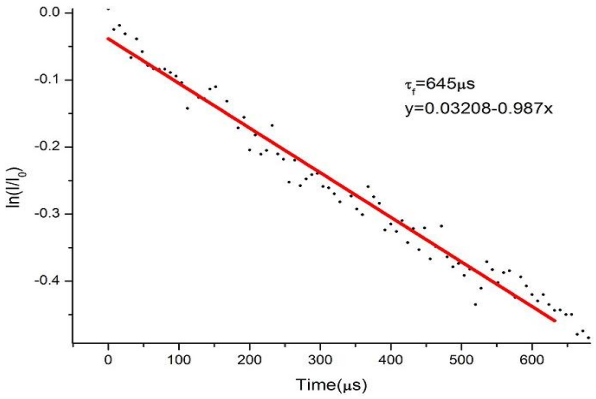

Fig. 6. Fluorescence decay curve of Er^{3+}:$(Sr_{0.7}Ca_{0.3})_3Y(BO_3)_3$ crystal corresponding to the $^4I_{13/2}\rightarrow{}^4I_{15/2}$ transition excited with 521nm laser radiation at room temperature.

Table 1 lists the main spectral parameters of Er^{3+}:$(Sr_{0.7}Ca_{0.3})_3Y(BO_3)_3$ crystal and some other Er^{3+}-doped crystal. In comparison with Er^{3+}:$Sr_3Y(BO_3)_3$ crystal, the Er^{3+}:$(Sr_{0.7}Ca_{0.3})_3Y(BO_3)_3$ crystal has large oscillator strength parameters Ω_t and emission cross-section (see Table 1). The large value of Ω_2 mainly originates from the absorption of the hypersensitive transition of $^4I_{15/2}\rightarrow{}^4G_{11/2}$ and $^4I_{15/2}\rightarrow{}^2H_{11/2}$. The stimulated emission cross-sections $\sigma_{em}(\lambda)$ of Er^{3+}:$(Sr_{0.7}Ca_{0.3})_3Y(BO_3)_3$ crystal is larger than that of Er^{3+}:$Sr_3Y(BO_3)_3$ and the other Er^{3+}-doped crystals (see Table 1). The quantum efficiency η_c of Er^{3+}:$(Sr_{0.7}Ca_{0.3})_3Y(BO_3)_3$ crystal is larger than that (7.9%) of Er^{3+}:$(Sr_{0.7}Ca_{0.3})_3Y(BO_3)_3$ crystal [23]. In a word, the spectral properties of Er^{3+}:$(Sr_{0.7}Ca_{0.3})_3Y(BO_3)_3$ crystal are than of Er^{3+}:$Sr_3Y(BO_3)_3$ crystal. The good spectral properties of Er^{3+}:$(Sr_{0.7}Ca_{0.3})_3Y(BO_3)_3$ crystal were caused by its structure disorder. When the Ca^{2+} ions partly were substituted for Sr^{2+} ion in $Sr_3Y(BO_3)_3$ crystal to form $(Sr_{0.7}Ca_{0.3})_3Y(BO_3)_3$ solid state, it resulted in the structure disorder of $(Sr_{0.7}Ca_{0.3})_3Y(BO_3)_3$ crystal [14]. It generally believes that the disorder structure can improve the spectral properties of crystal materials [27, 28].

4. Conclusion

Er^{3+}:$(Sr_{0.7}Ca_{0.3})_3Y(BO_3)_3$ crystal has been successfully grown by the Czochralski method. In comparison with Er^{3+}:$Sr_3Y(BO_3)_3$ crystal, the spectral properties of Er^{3+}:$(Sr_{0.7}Ca_{0.3})_3Y(BO_3)_3$ crystal have been greatly improved, such as large oscillator strength parameters Ω_t,

large stimulated emission cross-sections $\sigma_{em}(\lambda)$ and high quantum efficiency η_c. Therefore, above results shows that after the Ca^{2+} ion partly substitute for Sr^{2+} ion in $Sr_3Y(BO_3)_3$ crystal to form the $(Sr_{0.7}Ca_{0.3})_3Y(BO_3)_3$ solid solution, it can improve the spectral properties of Er^{3+}:$(Sr_{0.7}Ca_{0.3})_3Y(BO_3)_3$ crystal. Therefore, Er^{3+}:$(Sr_{0.7}Ca_{0.3})_3Y(BO_3)_3$ crystal may be regarded as a 1.55 μm laser gain medium candidate.

Acknowledgements

This work is supported by the National Natural Science Foundation of China (No. 61108054) and the National Natural Science Foundation of Fujian Province (No. 2011J01376), respectively.

References

[1] J. A. Capobianco, P. Kabro, F. S. Ermeneux, R. Moncorgé, M. Bettinelli, E. Cavalli, Chem. Phys. **214**, 329 (1997).
[2] P. Le Boulanger, J. -L. Doualan, S. Girard, J. Margerie, R. Moncorgé, Phys. Rev. B **60**, 11380(1999).
[3] A. A. Kaminskii, V. S. Mironov, A. Kornienko, S. N. Bagaev, G. Boulon, A. Brenier, B. Di Bartolo, Phys. Stat. Sol. (a) **151**, 231(1995).
[4] M. C. Pujol, M. Rico, C. Zaldo, R. Solé, V. Nikolov, X. Solans, M. Aguiló, F. Díaz, Appl. Phys. B **68**, 187 (1999).
[5] X. M. Han, G. F. Wang, Taiju Tsuboi, J. Crystal. Growth **242**, 412 (2002).
[6] X. Z, Li, Z. B. Lin, L. Z. Zhang, G. F. Wang, J. Crystal Growth **293**, 157 (2006).
[7] P.-H. Haumesser, R. Gaumé, J.-M. Benitez, B. Viana, B. Ferrand, G. Aka, A. Vivien, J. Crystal Growth **233**, 242 (2001).
[8] F. Druon, S. Chénais, P. Raybaut, F. Balembois, P. Georges, R. Gaumé, G. Aka, B. Vianna, S. Mohr, D. Kopf, Opt. Lett. **27**, 197 (2002).
[9] S. Chénais, F. Druon, F. Balembois, P. Georges, R. Gaume, P.-H. Haumesser, B. Vianna, G. Aka, D. Vivien, J. Opt. Soc. Am. B **19**, 1083 (2002).
[10] J. G. Pan, Z. S. Hu, Z. B. Lin, G. F. Wang, J. Crystal Growth **260**, 456 (2004).
[11] D. Zhao, Z. S. Hu, Z. B. Lin, G. F. Wang, J. Crystal Growth **277**, 401 (2005).
[12] J. G. Pan, G. F. Wang, J. Crystal Growth **262**, 527 (2004).
[13] J. G. Pan, S. F. Wu, G. F. Wang, Opt. Mater. **28**, 391 (2006).
[14] R. Gaume, B. Viana, D. Vivien, J. P. Roger, D. Fournier, J. P. Souron, Opt. Mater. **24**, 385 (2003).
[15] D. Zhao, Z. B. Lin, L. Z. Zhang, G. F. Wang, J. Lumin. **130**, 424 (2010).
[16] B. R. Judd, Phys. Rev. **127**, 750 (1962).
[17] G. S. Ofelt, J. Chem. Phys. **37**, 511 (1962).
[18] W. Zhao, W. W. Zhou, M. J. Song, G. F. Wang, J. M. Du, H. J. Yu, Optoelectron. Adv. Mater.-Rapid. Commun. **5**(1), 49 (2011).
[19] Y. X. Zhao, Y. S. Huang, L. Z. Zhang, Z. B. Lin, G. F. Wang, Optoelectron. Adv. Mater.-Rapid. Commun. **6**(3-4), 357 (2012).
[20] B. Xiao, L. Z. Zhang, Z. B. Lin, Y. S. Huang, G. F. Wang, Optoelectron. Adv. Mater.-Rapid. Commun. **6**(3-4), 404 (2012).
[21] B. F. Aull, H. P. Jenssen, IEEE J. Quantum Eletron. **QE-18**, 925 (1982).
[22] P. J. Deren, R. Mahiou, Opt. Mater. **29**, 766 (2007).
[23] B. Simondi-Teisseire, B. Viana, D. Vivien, A. M. Lejus, Phys. Stat. Sol. (a) **155**, 249 (1996).
[24] D. K. Sardar, W. M. Bradley, J. J. Perez, J. Appl. Phys. **93**, 260 (2003).
[25] Y. J. Chen, X. Q. Lin, Z. D. Luo, Y. D. Huang, Opt. Mater. **27,** 625 (2004).
[26] B. Wei, Z. B. Lin, L. Z. Zhang, G. F. Wang, J. Phys. D: Appl. Phys. **40**, 2792 (2007).
[27] B. Xiao, Y. S. Huan, L. Z. Zhang, Z. B. Lin, G. F. Wang, RSC Adv. **2**, 5271 (2012).
[28] X. M. Meng, Z. B. Lin, L. Z. Zhang, Y. S. Huang, G. F. Wang, CrystEngComm **13**, 4069 (2011).

*Corresponding author: wgf@ms.fjirsm.ac.cn